

# Biomimetic Complexes of Co(II), Mn(II), and Ni(II) with 2-Propyl-4,5-imidazoledicarboxylic Acid. EGA–MS Characterization of the Thermally Induced Decomposition<sup>1</sup>

R. Risoluti, G. Gullifa, M. A. Fabiano, and S. Materazzi

Department of Chemistry, “Sapienza” University of Rome, p. le A. Moro 5, Rome, 00185 Italy  
e-mail: stefano.materazzi@uniroma1.it

Received April 24, 2015

**Abstract**—Solid complexes of Co(II), Mn(II), and Ni(II) with 2-propyl-4,5-imidazoledicarboxylic acid have been prepared and studied by means of mass spectrometry evolved gas analysis (EGA–MS). The applied hyphenated thermoanalytical approach has allowed description of the thermally induced decomposition steps and has supported the suggested mechanism. The results of this work in combination with the earlier reported data have suggested that two main thermally induced decomposition pathways are common of the imidazole-substituted complexes.

**Keywords:** 2-propyl-4,5-imidazoledicarboxylic acid, biomimetic complex, cobalt, nickel, manganese, evolved gas analysis, TG–MS

**DOI:** 10.1134/S1070363215100242

Metal complexes containing imidazoledicarboxylate ligands have been widely investigated in view of their diverse structure and topology [1–3] allowing for versatile promising applications in the fields of gas storage, catalysis, optoelectronics, sensors, magnetism, luminescence, and porous materials [4–14].

The available reports generally discuss the complexes synthesis and characterization by means of elemental analysis, IR spectroscopy, and (sometimes) NMR spectroscopy. Thermal analysis has been recently applied for elucidation of the thermally induced decomposition mechanism [4, 7–9, 11, 13] in addition to well developed X-ray diffraction approaches [5, 6, 10, 12]. However, thermogravimetry alone is not always sufficient to derive the detailed reaction mechanism; in view of this, the hyphenated thermal analysis and FTIR or MS spectroscopy techniques have been applied to describe the decomposition steps and to elucidate the complexes decomposition mechanism (cf. reviews [15–19] and references therein).

The TGA–MS studies of the imidazole-substituted complexes conducted in our group have revealed the

systematic similarity of the complexes decomposition pathways. Experimental evidences [20–27] generally showed low-temperature decomposition steps assigned to the loss of water and of the counter ions, while the subsequent decomposition followed one of the two pathways, depending on the ligand structure. In the case of *N,N'*-bis(2-hydroxybenzylidene)-1,1-diaminobutane [20], 2-aminomethylbenzimidazole [21], or imidazole-4,5-dicarboxylic acid [22, 23], the ligand is eliminated and/or chemically transformed, as confirmed by the mass loss data and analysis of the evolved gas products. On the contrary, with bis(1-methylimidazol-2-yl)ketone [24–26] or dopamine [27] as ligand, the 1 : 2 or 1 : 4 complex remained stable till the final decomposition stage, the latter yielding the metal oxide.

In this study, solid complexes of Co(II), Mn(II), and Ni(II) with 2-propyl-4,5-imidazoledicarboxylic acid (H<sub>2</sub>PIDC) were prepared and characterized, and their decomposition was studied via simultaneous TGA and MS of the evolved gases (the hyphenated TGA–EGA–MS technique).

Elemental analysis of the prepared complexes (Table 1) confirmed the suggested composition of the

<sup>1</sup> The text was submitted by the authors in English.

**Table 1.** Elemental analysis data of the prepared complexes

Complex	Found, %				Calculated, %			
	C	H	N	metal	C	H	N	metal
Co(H <sub>2</sub> PIDC) <sub>2</sub> (H <sub>2</sub> O) <sub>2</sub>	39.0	4.4	11.6	12.3	39.3	4.5	11.4	12.1
Ni(H <sub>2</sub> PIDC) <sub>2</sub> (H <sub>2</sub> O) <sub>2</sub>	39.2	4.3	11.3	12.1	39.3	4.5	11.4	12.1
Mn(H <sub>2</sub> PIDC) <sub>2</sub> (H <sub>2</sub> O) <sub>2</sub>	34.2	4.9	09.9	11.1	34.4	5.0	10.0	11.3

**Table 2.** Temperature range of the main stages of thermal decomposition of the complexes and the corresponding mass loss

Complex	First stage: 100–190°C		Second stage: 230–300°C		Third stage: 300–450°C	
	found, %	calculated, %	found, %	calculated, %	found, %	calculated, %
Co(H <sub>2</sub> PIDC) <sub>2</sub> (H <sub>2</sub> O) <sub>2</sub>	13.3	13.1	45.0	45.8	25.7	26.0
Ni(H <sub>2</sub> PIDC) <sub>2</sub> (H <sub>2</sub> O) <sub>2</sub>	13.0	13.1	46.9	45.8	24.0	26.0
Mn(H <sub>2</sub> PIDC) <sub>2</sub> (H <sub>2</sub> O) <sub>2</sub>	13.6	13.2	46.0	46.3	26.3	26.2

products, since the experimentally determined elements content coincided with the calculated values.

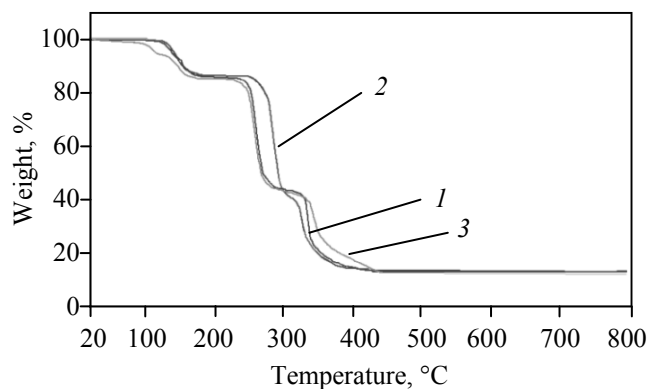
FTIR spectra of the products contained the following common absorption bands: 2975 (m), 1720 (s), 1540 (s), 1390 (s), 1280 (s), 1100 (m), 860 (m), 775 (m), 695 (w), 660 (m), and 510 (m) cm<sup>-1</sup>. The spectral features were in accordance with the earlier reported by Yang et al. for similar complexes [28].

Figure 1 displays TGA curves of the studied complexes decomposition recorded upon heating in air. For all the compounds, thermal decomposition process consisted of three main steps.

The corresponding mass loss (Table 2) and the complexes composition (Table 1) suggested that the first decomposition step consisted in elimination of the hydrate water molecules and the side chain of one of the ligands. The suggested mechanism coincided with the molecular structure of similar complexes (cf. Figs. 2b, 3b, and 4c in [30]): the side chain in the external position should be eliminated easier than the other one. Additional confirmation of the suggested mechanism validity was obtained via mass spectrometry analysis of the evolved gases. In particular, elimination of water was marked by the signals at  $m/z = 17$  and  $18$ , whereas elimination of the side chain fragment was assigned to the signal at  $m/z = 28$  (Fig. 2). The features of the complexes thermal decomposition remained practically the same when the analysis was conducted under inert atmosphere (N<sub>2</sub>).

The second decomposition step was clarified in the experiment under inert atmosphere. The presence of the signals at  $m/z = 28$ ,  $29$ , and  $46$  (Fig. 2) and the corresponding mass loss (Table 2) evidenced about rupture of the ligand ring as depicted in Fig. 3, followed by the structure rearrangement. The final decomposition step led to deep burning-out of the organic part of the complex yielding the metal oxide as the high-temperature residue.

In summary, the obtained results clearly revealed that the studied metal complexes with 2-propyl-4,5-imidazoledicarboxylic acid belonged to the first group according to the classification mentioned in the introduction; that is, their thermal decomposition presumed formation of the well-detected intermediate



**Fig 1.** TGA curves of (1) Co(H<sub>2</sub>PIDC)<sub>2</sub>(H<sub>2</sub>O)<sub>2</sub>, (2) Ni(H<sub>2</sub>PIDC)<sub>2</sub>(H<sub>2</sub>O)<sub>2</sub>, and (3) Mn(H<sub>2</sub>PIDC)<sub>2</sub>(H<sub>2</sub>O)<sub>2</sub> recorded under air flow of 100 mL/min at heating rate of 5 deg/min.

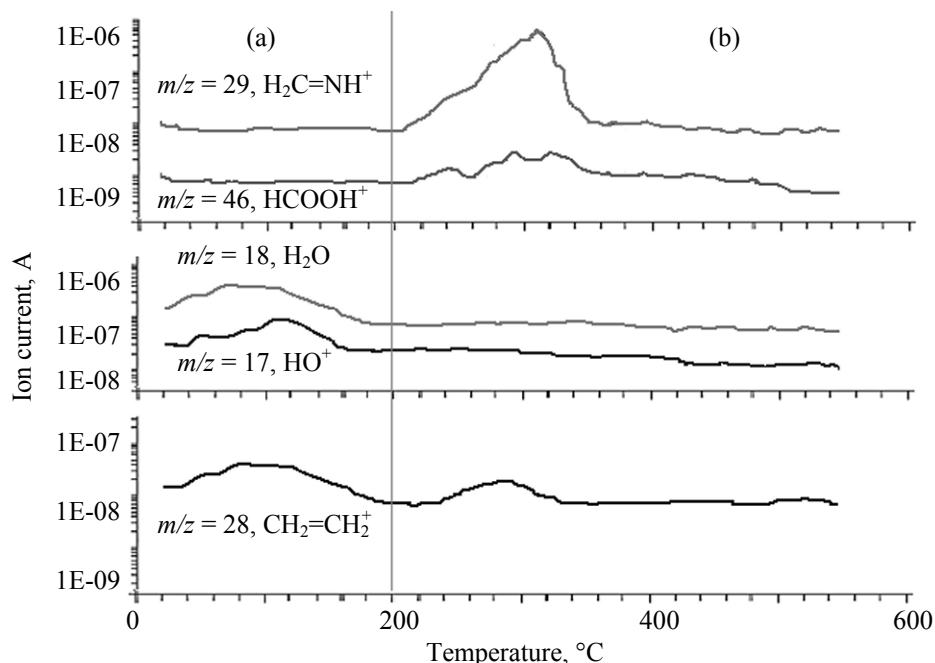


**Fig. 2.** Mass spectroscopy analysis of the evolved gaseous products during the complexes decomposition: (a) first TGA step and (b) second + third TGA step. The  $m/z$  profiles were the same for all the analyzed complexes.

containing a five- or six-membered ring further decomposing into the corresponding metal oxide.

### EXPERIMENTAL

2-Propyl-4,5-imidazoledicarboxylic acid as well as cobalt, nickel and manganese chlorides (Aldrich or Merck, A.R. grade) were used as received. The conditions of each synthesis to precipitate the complexes of general formula  $M(H_2PIDC)_2(H_2O)_2$ , where  $M=Co(II)$ ,  $Ni(II)$  or  $Mn(II)$ , reported in [28] were strictly followed. Elemental analysis was performed using a VarioEl III CHN Analyzer

instrument. FTIR spectra (KBr pellets) were recorded using a 1760X (Perkin-Elmer) instrument. The metals concentration was determined using an ICP-OES instrument (Varian ICP/VISTA MPX) equipped with an ultrasonic nebulizer (U 5000 AT+, Cetac Technologies Inc.). The analysis of the metal content was performed in six replicates; the results were averaged, and the signal detected for the blank specimen under the same conditions was subtracted. To account for the nebulizer efficiency, internal reference (100  $\mu g/L$  of yttrium,  $\lambda = 371.030$  nm) was used.

TGA curves were recorded using a TGA7 (Perkin-Elmer) instrument. The analysis was run under the conditions used in the earlier studies [29, 30]: specimen mass 7–8 mg, platinum crucible, temperature range of 20–850°C, heating at 5 deg/min (allowing for the best stages resolution at a reasonable experiment duration), 100% nitrogen or a 4 : 1 v/v mixture of nitrogen and oxygen at a flow rate of 100 mL/min.

The hyphenated TGA–MS experiment was performed taking advantage of a STD 2960 synchronous DTA–TGA instrument (TA Instruments) using sealed crucibles with a pinhole at the top. The gaseous species were analyzed using a ThermoStar GDS 200 (Balzers Instrument) quadrupole mass spectrometer equipped

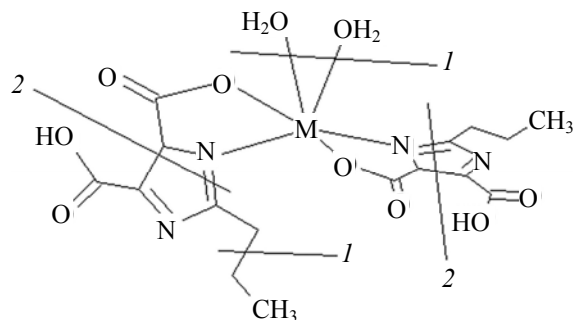


**Fig. 3.** Scheme of the general decomposition mechanism: (1) bonds rupture at the first decomposition step and (2) bonds rupture at the second decomposition step.

with Chaneutron detector (EI, 70 eV) connected via a heated 100% methyl deactivated fused silica capillary tubing. The TGA curves recorded using the two instruments gave reproducible results.

### ACKNOWLEDGMENTS

Authors acknowledge the assistance of Dr. L.W. Wo in the synthesis of the complexes.

### REFERENCES

1. Rajendiran, T.M., Kirk, M.L., Setyawati, I.A., Caudle, M.T., Kampf, J.W., and Pecoraro, V.W., *Chem. Commun.*, 2003, p. 824. DOI: 10.1039/B212684M.
2. Bayon, J.C. and Net, G., *J. Chem. Soc. Dalton Trans.*, 1987, p. 3003.
3. Zou, R.-Q., Sakurai, H., and Xu, Q., *Angew. Chem. Int. Ed.*, 2006, vol. 45, p. 2542 DOI: 10.1002/ange.200503923.
4. Crea, F., Falcone, G., Foti, C., and Giuffrè, O., *New J. Chem.*, 2014, vol. 38(8), p. 3973. DOI: 10.1039/C4NJ00830H.
5. Liu, Y., Kravtsov, V.C., and Eddaoudi, M., *Angew. Chem. Int. Ed.*, 2008, vol. 47, p. 8446 DOI: 10.1002/anie.200802680.
6. Wang, S., Zhang, L., Li, G., Huo, Q., and Liu, Y., *Cryst. Eng. Comm.*, 2008, vol. 10, p. 1662. DOI: 10.1039/B812782B.
7. Serra Moreno, J., Panero, S., Martinelli, A., Sabbieti, M.G., and Agas, D., *J. Biomedical Mat. Res: Part A*, 2009, vol. 88, p. 832. DOI: 10.1002/jbm.a.32230.
8. Liu, Y., Kravtsov, V., Walsh, R.D., Poddar, P., Srikanth, H., and Eddaoudi, M., *Chem. Commun.*, 2004, p. 2806. DOI: 10.1039/B409459J.
9. Perrino, C., Marconi, E., Tofful, L., Farao, C., and Canepari, S., *Atmospheric Environment*, 2012, vol. 54, p. 36. DOI: 10.1016/j.atmosenv.2012.02.078.
10. Yue, S., Li, N., Bian, J., Hou, T., and Ma, J., *Synthetic Metals*, 2012, vol. 162, p. 247. DOI: 10.1016/j.synthmet.2011.11.030.
11. Bevilacqua, M., Bucci, R., and Marini, F., *Food Chem.*, 2013, vol. 140, p. 726. DOI: 10.1016/j.foodchem.2012.11.018.
12. Liu, Y., Kravtsov, V., Larsena, R., and Eddaoudi, M., *Chem. Commun.*, 2006, p. 1488. DOI: 10.1039/B600188M.
13. Migliorati, V., Ballirano, P., Gontrani, L., Ceccacci, F., and Caminiti, R., *J. Phys. Chem. B*, 2013, vol. 117, p. 7806. DOI: 10.1021/jp403103w.
14. Nouar, F., Eckert, J., Eubank, J.F., Forster, P., and Eddaoudi, M., *J. Am. Chem. Soc.*, 2009, vol. 131, p. 2864. DOI: 10.1021/ja807229a.
15. Materazzi, S. and Risoluti, R., *Appl. Spectr. Rev.*, 2014, vol. 49(8), p. 635. DOI: 10.1080/05704928.2014.887021.
16. Materazzi, S. and Vecchio, S., *Appl. Spectr. Rev.*, 2013, vol. 48, p. 654. DOI: 10.1080/05704928.2013.786722.
17. Materazzi, S. and Vecchio, S., *Appl. Spectr. Rev.*, 2011, vol. 46, p. 261. DOI: 10.1080/05704928.2011.565533.
18. Materazzi, S. and Vecchio, S., *Appl. Spectr. Rev.*, 2010, vol. 45, p. 241. DOI: 10.1080/05704928.2010.483664.
19. Materazzi, S., Gentili, A., and Curini, R., *Talanta*, 2006, vol. 69, p. 781. DOI: 10.1016/j.talanta.2005.12.007.
20. Materazzi, S., Risoluti, R., and Napoli, A., *Thermochim. Acta*, 2015, vol. 606, p. 90. DOI: 10.1016/j.tca.2015.03.009.
21. Materazzi, S., Risoluti, R., Finamore, J., and Napoli, A., *Microchem. J.*, 2014, vol. 115, p. 27. DOI: 10.1016/j.microc.2014.02.006.
22. Materazzi, S., Napoli, A., Finamore, J., Risoluti, R., and D'Arienzo, S., *Int. J. Mass Spectrom.*, 2014, vols. 365–366, p. 372. DOI: 10.1016/j.ijms.2014.03.013.
23. Materazzi, S., Foti, C., Crea, F., Risoluti, R., and Finamore, J., *Thermochim. Acta*, 2014, vol. 580, p. 7. DOI: 10.1016/j.tca.2014.01.025.
24. Vecchio, S., Materazzi, S., Wo, L.W., and De Angelis Curtis, S., *Thermochim. Acta*, 2013, vol. 568, p. 31. DOI: 10.1016/j.tca.2013.06.016.
25. Materazzi, S., Vecchio, S., Wo, L.W., and De Angelis Curtis, S., *Thermochim. Acta*, 2012, vol. 543, p. 183. DOI: 10.1016/j.tca.2012.05.013.
26. Materazzi, S., Vecchio, S., Wo, L.W., and De Angelis Curtis, S., *J. Therm. Anal. Calorim.*, 2011, vol. 103(1), p. 59. DOI: 10.1007/s10973-010-1137-6.
27. Bretti, C., Crea, F., De Stefano, C., Foti, C., and Vianelli, G., *J. Chem. Eng. Data*, 2013, vol. 58, p. 2835. DOI: 10.1021/je400568u.
28. Yang, Z., Chen, N., Wang, C., Yan, L., and Li, G., *Synthesis and Reactivity in Inorganic, Metal-Organic, and Nano-Metal Chemistry*, 2012, vol. 42, p. 336. DOI: 10.1080/15533174.2011.610770.
29. Materazzi, S., Vecchio, S., and De Angelis Curtis, S., *J. Therm. Anal. Calorim.*, 2013, vol. 112 (1), p. 529. DOI: 10.1007/s10973-012-2762-z.
30. Materazzi, S., De Angelis Curtis, S., Vecchio Cipriotti, S., Risoluti, R., and Finamore, J., *J. Therm. Anal. Cal.*, 2014, vol. 116(1), p. 93. DOI: 10.1007/s10973-013-3495-3.